AD-A184 293 EFFECTS OF PRESSURE FLUCTUATIONS ON NICKEL ELECTRODES 1/1
(U) AEROSPACE CORP EL SEGUNDO CA CHEMISTRY AND PHYSICS
LAB A H ZIMMERMAN 30 APR 87 TR-0086A(2945-01)-2
UNCLASSIFIED SD-TR-87-42 F04701-85-C-0086 F/G 9/1 NL

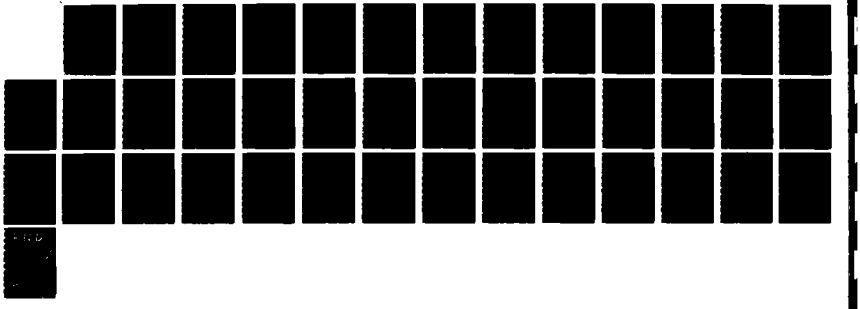

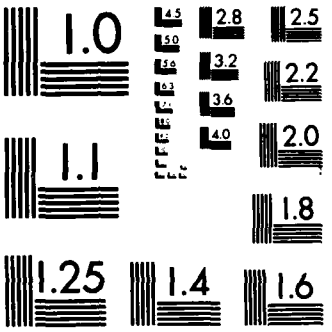

MICROCOPY RESOLUTION TEST CHART
NATIONAL BUREAU OF STANDARDS-1963-A

(12)

DTIC FILE COPY

REPORT SD-TR-87-42

AD-A184 293

Effects of Pressure Fluctuations on Nickel Electrodes

A. H. ZIMMERMAN
Chemistry and Physics Laboratory
Laboratory Operations
The Aerospace Corporation
El Segundo, CA 90245

30 April 1987

DTIC
ELECTE
SEP 1 0 1987
S D
CD

Prepared for

SPACE DIVISION
AIR FORCE SYSTEMS COMMAND
Los Angeles Air Force Station
P.O. Box 92960, Worldway Postal Center
Los Angeles, CA 90009-2960

APPROVED FOR PUBLIC RELEASE.
DISTRIBUTION UNLIMITED

87 9

This report was submitted by The Aerospace Corporation, El Segundo, CA 90245, under Contract No. F04701-85-C-0086 with the Space Division, P.O. Box 92960, Worldway Postal Center, Los Angeles, CA 90009-2960. It was reviewed and approved for The Aerospace Corporation by S. Feuerstein, Director, Chemistry and Physics Laboratory.

Lt Thomas Wetterstroem/CW was the project officer for the Mission-Oriented Investigation and Experimentation (MOIE) Program.

This report has been reviewed by the Public Affairs Office (PAS) and is releasable to the National Technical Information Service (NTIS). At NTIS, it will be available to the general public, including foreign nationals.

This technical report has been reviewed and is approved for publication. Publication of this report does not constitute Air Force approval of the report's findings or conclusions. It is published only for the exchange and stimulation of ideas.

Thomas Wetterstroem

THOMAS WETTERSTROEM, Lt, USAF
MOIE Project Officer
SD/CWASB

Joseph Hess

JOSEPH HESS, GM-15
Director, AFSTC West Coast Office
AFSTC/WCO OL-AB

UNCLASSIFIED

SECURITY CLASSIFICATION OF THIS PAGE

A184293

REPORT DOCUMENTATION PAGE

1a. REPORT SECURITY CLASSIFICATION Unclassified	1b. RESTRICTIVE MARKINGS
2a. SECURITY CLASSIFICATION AUTHORITY	3. DISTRIBUTION/AVAILABILITY OF REPORT Approved for public release; distribution unlimited.
2b. DECLASSIFICATION/DOWNGRADING SCHEDULE	
4. PERFORMING ORGANIZATION REPORT NUMBER(S) TR-0086A(2945-01)-2	5. MONITORING ORGANIZATION REPORT NUMBER(S) SD-TR-87-42
6a. NAME OF PERFORMING ORGANIZATION The Aerospace Corporation 6b. OFFICE SYMBOL (If applicable)	7a. NAME OF MONITORING ORGANIZATION Space Division
6c. ADDRESS (City, State, and ZIP Code) El Segundo, CA 90245	7b. ADDRESS (City, State, and ZIP Code) Los Angeles Air Force Station Los Angeles, CA 90009-2960
8a. NAME OF FUNDING/SPONSORING ORGANIZATION 8b. OFFICE SYMBOL (If applicable)	9. PROCUREMENT INSTRUMENT IDENTIFICATION NUMBER F04701-85-C-0086-P00016
8c. ADDRESS (City, State, and ZIP Code)	10. SOURCE OF FUNDING NUMBERS PROGRAM ELEMENT NO. / PROJECT NO. / TASK NO. / WORK UNIT ACCESSION NO.

11. TITLE (Include Security Classification)

EFFECTS OF PRESSURE FLUCTUATIONS ON NICKEL ELECTRODES

12. PERSONAL AUTHOR(S)
Zimmerman, Albert H.

13a. TYPE OF REPORT	13b. TIME COVERED FROM ____ TO ____	14. DATE OF REPORT (Year, Month, Day)	15. PAGE COUNT
		1987 April 30	39

16. SUPPLEMENTARY NOTATION

17. COSATI CODES			18. SUBJECT TERMS (Continue on reverse if necessary and identify by block number)
FIELD	GROUP	SUB-GROUP	Nickel electrode, Pressure Nickel hydrogen Hydrogen Degradation

19. ABSTRACT (Continue on reverse if necessary and identify by block number)

The rapidly fluctuating pressure environment that exists in today's nickel-hydrogen battery cells during high rate charge/discharge operation can potentially act as an important source of stress to the active materials in the nickel electrodes. This study examines the coupling between the rapidly fluctuating pressure environment of the nickel-hydrogen cell and degradation of the nickel electrodes arising from expansion and contraction of the active materials. A model is developed to describe this coupling, and the sensitivity of the coupling to the parameters in the model is analyzed. The model is used to determine modes of nickel-hydrogen cell operation for which the pressure environment is particularly critical in terms of potential degradation. The results indicate that cell operation involving rapid cycling or quite large dynamic operating pressure ranges may cause significant stress to the nickel electrodes, and may be an important component in degradation and failure rates. Finally, cell tests are suggested that should allow the effect of the nickel-hydrogen cell pressure environment on performance to be determined.

20. DISTRIBUTION/AVAILABILITY OF ABSTRACT	21. ABSTRACT SECURITY CLASSIFICATION
☒ UNCLASSIFIED/UNLIMITED ☐ SAME AS RPT ☐ DTIC USERS	Unclassified
22a NAME OF RESPONSIBLE INDIVIDUAL	22b. TELEPHONE (Include Area Code) / 22c OFFICE SYMBOL

DD FORM 1473, 84 MAR

83 APR edition may be used until exhausted.
All other editions are obsolete.

SECURITY CLASSIFICATION OF THIS PAGE

UNCLASSIFIED

CONTENTS

Accesion For

NTIS CRA&I ☑

DTIC TAB ☐

Unannounced ☐

Justification

By

Distribution/

Availability Codes

Dist | Avail and/or Special

A-1

QUALITY INSPECTED 2

FIGURES

FIGURES (Continued)

TABLES

I. INTRODUCTION

Although it has generally been accepted that nickel electrodes perform about the same in nickel-hydrogen battery cells as in nickel-cadmium cells, increasing nickel-hydrogen battery usage has suggested some differences not previously recognized. For example, the effect of large, sometimes relatively rapid variations in hydrogen pressure in the nickel-hydrogen cell on the nickel electrode active material has not been adequately evaluated. Recent measurements of active material densities[1] indicate that the active material can undergo dynamic expansion and contraction as state of charge changes, and that at some states of charge the active material exists as a low density material having a large compressibility. This was found to be particularly true for nickel electrode active material containing 10% cobalt hydroxide, the level of this additive that is used in many nickel-hydrogen cell electrodes. The compressibility of the active material can allow expansion and contraction of the active material deposits in response to pressure fluctuations in the cell. This kind of expansion and contraction is generally recognized to be a source of stress on the sintered electrode structure[2] and on the morphology of the active material deposit in the pores of the sintered substrate.[3] Such stresses can lead to losses in dischargeable capacity or premature loss of sinter integrity over the course of long term cycling. Such concerns are of particular significance in some of the second generation nickel-hydrogen cells, which have employed extremely high operating pressure ranges (up to 1000 psi) to increase capacity and energy density.

The purpose of the work in this report is to model the response of the active material in nickel electrodes to the pressure fluctuations that can arise during the operation of a nickel-hydrogen cell. The model is then used to evaluate what pressure environments are likely to be a concern in terms of enhanced nickel electrode degradation. The applicability of the study to the nickel-hydrogen cell is determined by comparing the results with the limited data that exist pertaining to physical stress and movement of active material during cycling. Finally, the kinds of studies that could be done to

experimentally evaluate how pressure fluctuations can influence nickel electrode structure and performance are proposed.

II. MODEL DEVELOPMENT

A model that can determine how pressure fluctuations influence the structure and morphology of a solid system must have at least two areas of input. The first of these areas is the stimulus to the system, which consists of a time varying pressure profile $P_a(t)$. The second area is the response function of the system to pressure, including the effects of variables that may be dependent on pressure, such as the state of charge and solid-state structure of the active material. These two input areas may then be coupled to give the system response to the pressure changes. The system response may be determined at various levels. The first and most basic level involves modeling the microscopic response of individual grains of active material, while the second level involves modeling the solid-state response in terms of bulk active material properties such as volume and density. The second of these two approaches is adopted in this work as being more conveniently suited to evaluating relative stresses in nickel electrodes as a result of active material expansion and contraction.

A. SYSTEM STIMULUS

The system stimulus consists of the variation in pressure in a nickel-hydrogen cell with time as the cell is cycled. The pressure typically increases linearly with time during a constant current charge until the cell reaches 80-90% of full charge, after which the pressure rise begins to flatten out as overcharge begins and the cell asymptotically approaches full charge. The rate of pressure rise decreases as the cell goes into overcharge because the oxygen evolved from the nickel electrode during overcharge recombines on the platinum catalysts with the hydrogen evolved at the hydrogen electrode. During discharge at a constant current the pressure decreases linearly with time. Thus for a single cycle the pressure variation is divided into three regions, as indicated in Fig. 1: the charge, overcharge, and discharge regions. The figure also shows that the charge region terminates at time t_c, the overcharge region at time t_o, and the discharge region ends at time t_d. Similarly, the pressure at the end of the charge region is P_c and at the end

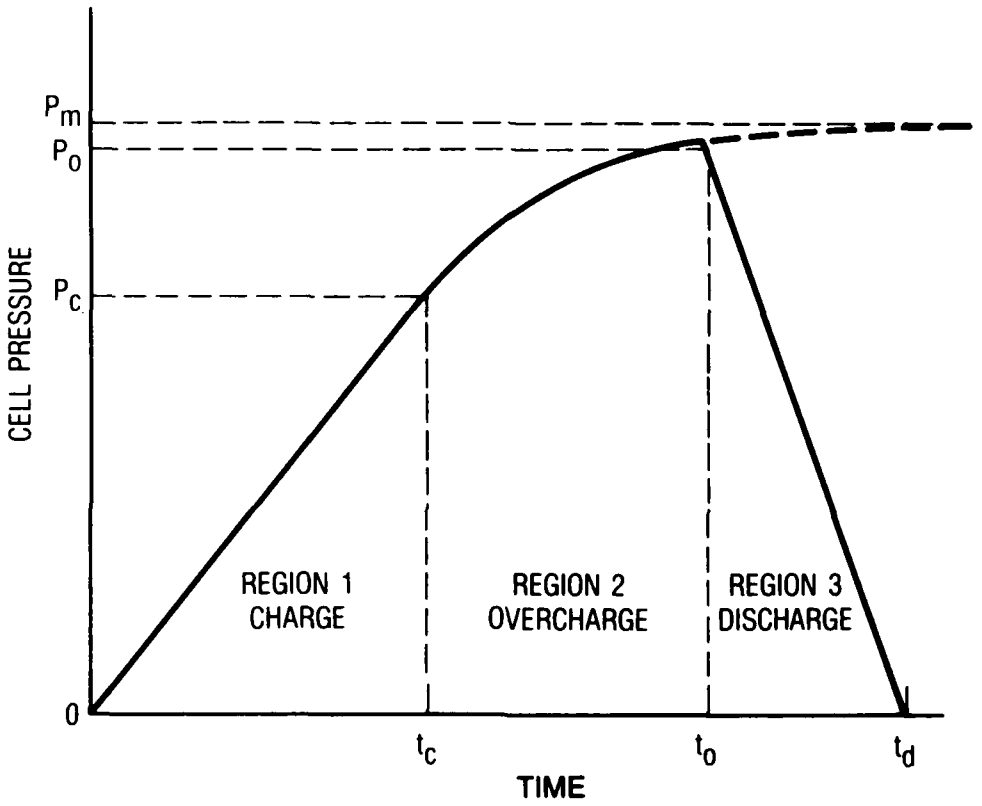

Figure 1. Model for NiH_2 Cell Pressure Cycle.

of the overcharge region the pressure is P_o. The pressure corresponding to full charge is P_m, and the pressure is assumed to be zero at the end of discharge and at the beginning of charge. The variation of pressure during a single cycle is represented analytically by the expression in Eq. (1).

$$\begin{aligned} P(t) &= P_c t/t & 0 \le t < t_c \\ P(t) &= P_m - (P_m - P_c)\exp(-(t-t_c)/b_m) & t_c \le t < t_o \\ P(t) &= P_o(t_d - t)/(t_d - t_o) & t_o \le t < t_d \end{aligned} \tag{1}$$

In Eq. (1) P_o is determined by the requirement for the pressure to asymptotically approach P_m, while the time constant b_m is determined by the requirement that the slope of the pressure be continuous at t_c. These constants are given by Eqs. (2) and (3), respectively.

$$P_o = P_m - (P_m - P_c)\exp(-(t_o - t_c)/b_m) \tag{2}$$

$$b_m = t_c(P_m - P_c)/P_c \tag{3}$$

The time-dependent pressure in the nickel-hydrogen cell $P_a(t)$, which varies periodically over m charge/discharge cycles, may be analytically expressed by Eq. (4) as the convolution of the pressure P(t) during a single cycle with the replicating function III(t) that is defined in Eq. (5) in terms of the Dirac delta function.

$$P_a(t) = III(t) * P(t) = \int_0^{\infty} III(x)P(t-x)dx \tag{4}$$

$$III(t) = \sum_{n=0}^{m} \delta(t - nt_d) \tag{5}$$

B. SYSTEM RESPONSE FUNCTION

The system response function that has been used in this study involves the response of the active material density or volume to changes in applied pressure, as well as the changes in volume that are known to accompany changes in cell state of charge.[1] The compressibility of the active material due to an externally applied pressure is taken from Ref. 1, and consistent with this previous work an exponential response of active material volume to a change in pressure is used having a time constant b_a. The work of Ref. 1 indicates this time constant to be on the order of 5-10 minutes for active material in operating nickel electrodes. This time constant arises from the physical capacity of the active material to incorporate gas into grain boundaries, microscopic intergrain voids, and surface adsorption. Therefore, the pressure in the interior of the active material deposit P_s will tend to lag the pressure exterior to the nickel electrode P_a during periods when the exterior pressure is changing rapidly relative to b_a.

Based on the data from Ref.1 for active nickel electrode materials containing 10% cobalt, the volume of the active material is assumed to exist in two limiting states, as indicated in Fig. 2. The low volume state is approached relatively slowly through annealing processes that occur at lower states of charge or in the absence of appreciable electrochemical activity. The active material can undergo a transition to a high volume state as it goes above states of charge from 0.7 to 0.8, i.e., as it approaches the overcharge condition. The volume changes indicated in Fig. 2 to occur with changes in state of charge may be combined with the changes due to time and pressure differentials to give the active material volume.

$$V(t) = 0.5A[1 + \tanh(-AP_d(t)/8.0)] \exp(-T/b_r) + V_i \qquad (6)$$

In Eq. (6) V_i is the minimum active material volume that can be attained at a given state of charge, and which can only be reached by extremely high compression or by allowing the material to stand for long periods of time without electrochemical activity. The time constant b_r defines the rate of approach to the low volume state in the absence of electrochemical charging

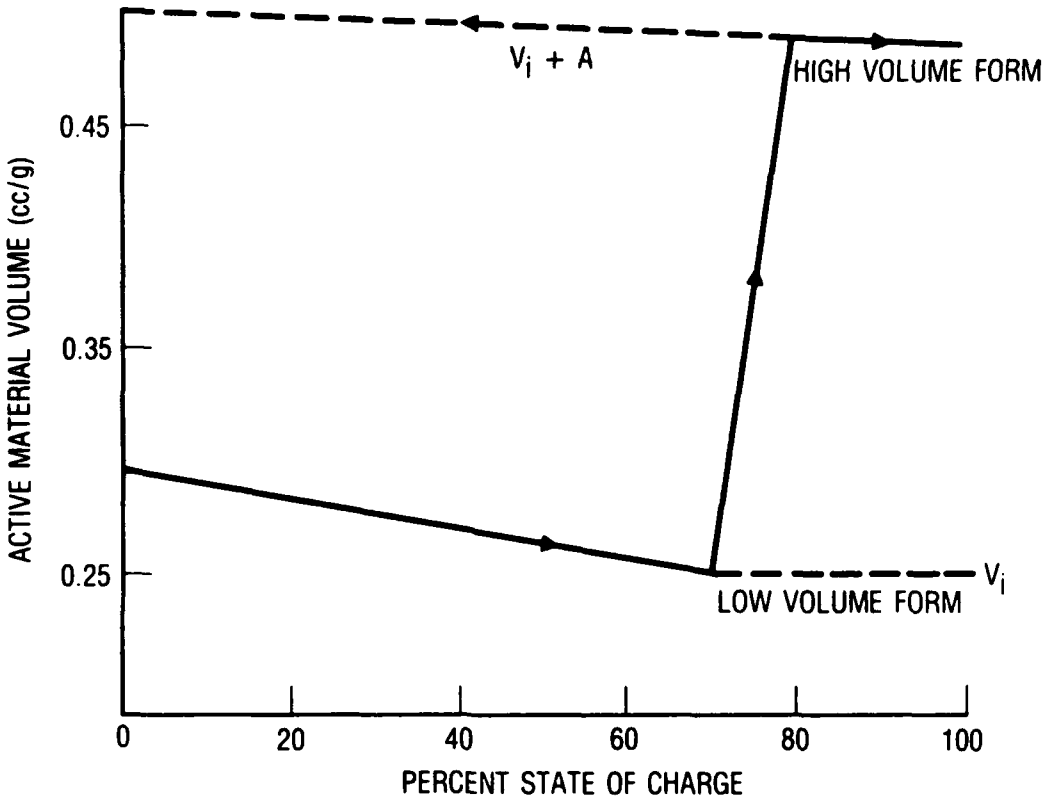

Figure 2. Active Material Volume as Function of State of Charge in Nickel Electrodes (Based on Data from Ref. 1)

activity, and T is the time elapsed since such charging activity. The function A in Eq. (6) indicates the difference between the high and the low volume states of the active material at any state of charge as indicated in Fig. 2. The constant 8.0 in Eq. (6) is a compressibility scale factor obtained from data in Ref. 1, and which scales the response of the volume to the applied pressure. The pressure P_d is a function of time and is the pressure differential between the interior and the exterior of the active material, as indicated by

$$P_d(t) = P_a(t) - P_s(t) \tag{7}$$

where $P_a(t)$ is the exterior pressure given by Eq. (4) and $P_s(t)$ is the interior pressure that is determined in the following section. It is assumed in the form of Eq. (6) that the volume of the active material can expand or contract in response to P_d, and that the maximum volume is limited by the total volume in the sinter structure while the minimum volume is limited by V_i. The tanh function in Eq. (6) provides an exponential asymptotic approach to these volume limits at low or high pressures, respectively. This treatment therefore does not deal with the expulsion of active material from the sinter structure, which can become possible at large negative pressures P_d when the sinter volume approaches a completely filled state.

C. DETERMINATION OF P_s

The average pressure in the interior of the active material deposit P_s is given by

$$P_s(t)b_a = P_a(t) * H(t)\exp(-t/b_a) = \int_0^\infty P_a(x)H(t-x)\exp[-(t-x)/b_a]dx \tag{8}$$

In Eq. (8), H(t) is the Heaviside function defined as 1 for t greater than or equal to zero, and otherwise zero. The convolution integral on the right hand side of Eq. (8) can be analytically evaluated, giving the expression in Eq. (9).

$$P_s(t)b_a = \sum_{n=0}^{m} \{H[t-(nt_d+t_c)]P_c A_n(t,nt_d,t_c)/t_c$$

$$+ H[t-(nt_d+t_o)] [P_m B_n(t,nt_d+t_c,t_o) - (P_m-P_c)C_n(t,nt_d+t_c,t_o)]$$

$$+ (P_o/(t_d-t_o)H(t-(n+1)t_d[t_d B_n(t,nt_d+t_o,t_d) - A_n(t,nt_d+t_o,t_d)]\} \quad (9)$$

The integrals A_n, B_n, and C_n in Eq. (9) are given by Eqs. (10)-(12), respectively.

$$A_n(t,g-nt_d,h-nt_d) = \int_g^h (x-nt_d) \exp[-t(t-x)/b_a]H(t-h)dx \quad (10)$$

$$B_n(t,g-nt_d,h-nt_d) = \int_g^h H(t-h) \exp[-(t-x)/b_a]dx \quad (11)$$

$$C_n(t,g-nt_d,h-nt_d) = \int_g^h H(t-h) \exp[-(x-t_c-nt_d)/b_m + (t-x)/b_a]dx \quad (12)$$

The definite integrals in Eqs. (10)-(12) are readily evaluated by removing the Heaviside functions from the integrals and treating them either as constants or as modifications to the limits of integration, depending on the limits of integration relative to the zero for the argument of the Heaviside function.

D. SUMMARY

A model has been developed in this section that allows the changes in bulk volume or density of a material to be determined in response to time-dependent variations in applied pressure. To model the volume variations of nickel electrode active material in a nickel-hydrogen battery cell, a time-dependent pressure is assumed that takes the form of Eq. (4), and the response of the active material to the pressure change is assumed to follow Eq. (6) and Fig. 2. The volume response defined by Eq. (6) depends on a number of parameters that may vary significantly with electrode operational conditions or life. The results in the following section first examine the sensitivity of the model developed here to the various parameters employed in the model.

Following this parametric study the model is applied to evaluating the actual volume changes that may be expected to occur during the typical modes of operation employed for nickel-hydrogen battery cells.

III. RESULTS

A. PARAMETRIC EVALUATION

In evaluating how the various parameters employed in the model of the previous section affect the overall active material expansion and contraction during cycling of nickel electrodes, a cumulative measure of such volume changes during cycling must be calculated. Such a cumulative volume change parameter was calculated by integrating the absolute value of the time derivative of the volume obtained from Eq. (6), with the time period of integration encompassing three full charge/discharge cycles. The integrated volume change calculated in this manner was used in the following parametric evaluations to indicate how sensitive the model is to each parameter, and is expressed in normalized form as cubic centimeters (cc) of total expansion or contraction during the three cycles per cc of active material in the nickel electrode.

The dependence of the volume changes arising from hydrogen pressure fluctuations on the maximum nickel-hydrogen cell operating pressure is indicated in Fig. 3 for various depths of discharge. Values for the other parameters used in the simulation of Fig. 3 are indicated in Table 1, where P_{off} is used to define the minimum pressure reached at the end of discharge. These results show that the volume changes are strong functions of both cell operating pressure and depth of discharge, both of which directly influence the rate of pressure change in a nickel-hydrogen cell for a given set of operating conditions. The leveling off in Fig. 3 of the integrated volume change at high operating pressures is a result of complete filling of the nickel eletrode sinter structure during discharge at high operating pressures. For the conditions of Fig. 3, the cell operating pressures at which the curves begin to level off are indicative of pressures at which active material may begin to be forced from the sinter structure during cycling.

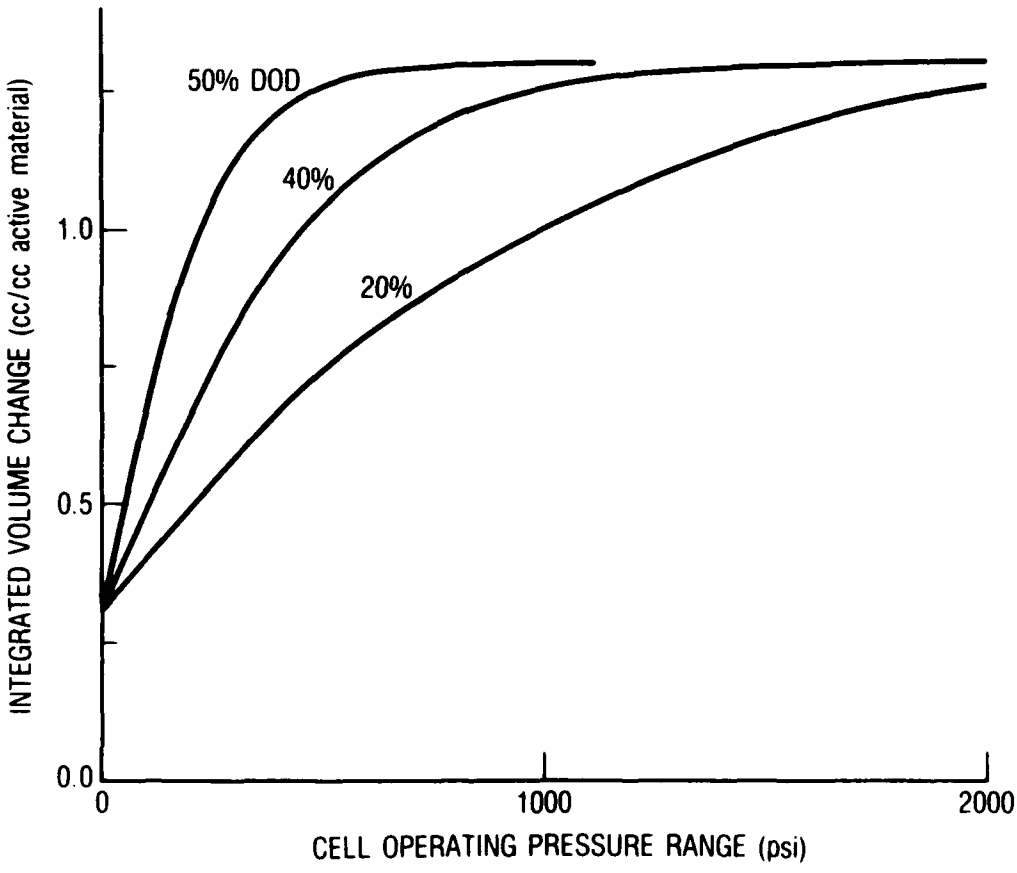

Figure 3. Integrated Volume Change of Nickel Electrode Active Material as a Function of Maximum NiH_2 Cell Operating Pressure, at Various Depths of Discharge.

Table 1. Simulation Parameters for Figures 3-8

	Fig 3	Fig 4	Fig 5	Fig 6	Fig 7	Fig 8
DOD	Variable	80%	80%	80%	80%	80%
t_c	0.75 hr	Variable	0.75	0.75	0.75	0.75
t_o	1.00 hr	Variable	1.00	1.00	1.00	1.00
t_d	1.50 hr	Variable	1.50	1.50	1.50	1.50
P_c	Variable	Variable	160 psi	160	160	160
P_m	Variable	Variable	200 psi	200	200	200
P_{off}	0.0 psi	0.0	0.0	0.0	0.0	0.0
V_i+A	0.5 cc/psi	0.5	0.5	0.5	0.0	Variable
b_r	24 hr	24	24	Variable	24	24
b_a	0.1 hr	0.1	0.1	0.1	Variable	0.1

The rate of hydrogen consumption and production in the nickel-hydrogen cell is directly proportional to discharge and charge rate, respectively. Figure 4 indicates how the integrated volume changes due to hydrogen pressure fluctuations depend on charge and discharge rate. The conditions of cycling modeled in Fig. 4 are indicated in Table 1. The results of Fig. 4 indicate that the volume change is sensitive to charge and discharge rate, with high rates of operation causing enhanced expansion and contraction of active material. At charge and discharge rates in excess of C/2 the volume changes begin again to level off due to expansion of the active material to fill (and potentially to be expelled from) the sinter structure. The volume changes arising during charge appear to be greater than those during discharge at a given rate.

The empirical expression given by Eq. (6) relates the active material volume to pressure differentials and time variations, and also includes

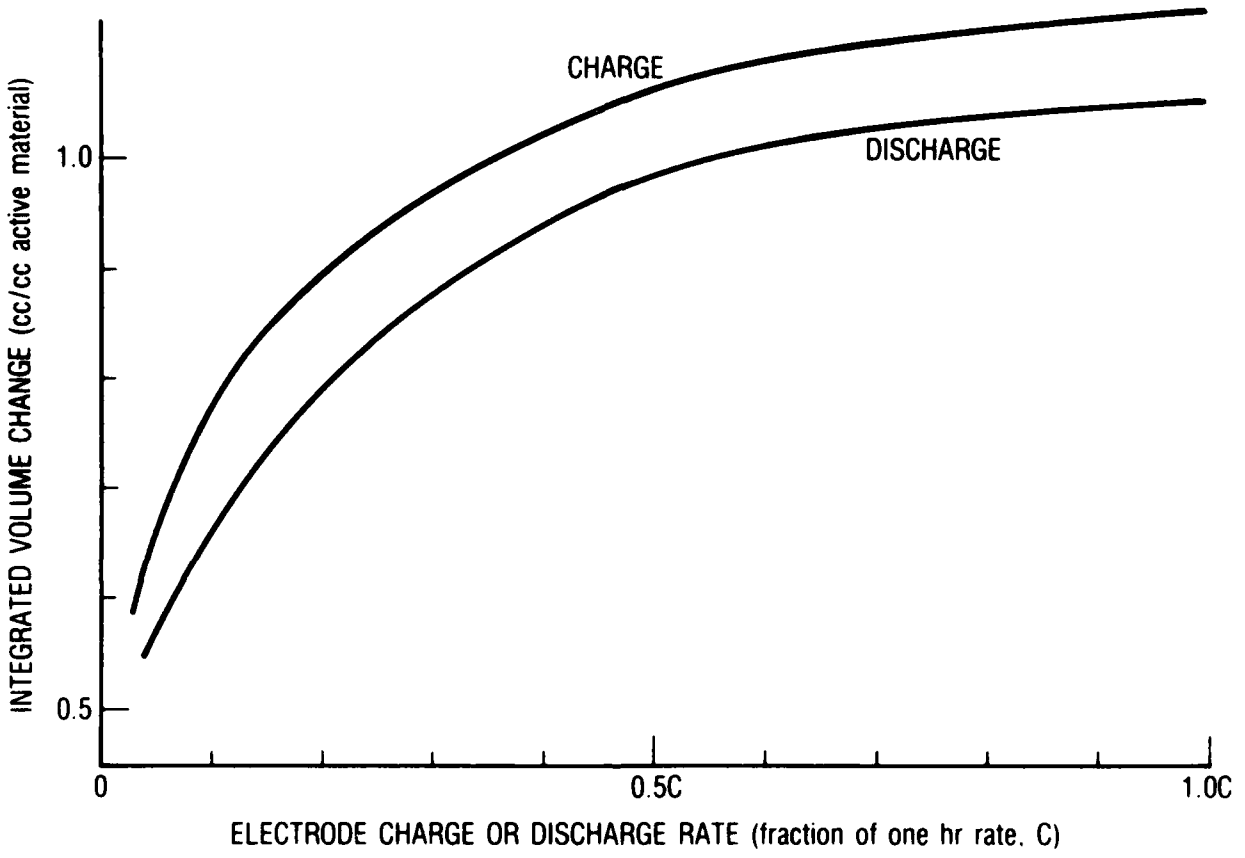

Figure 4. Integrated Changes in Volume for Nickel Electrode Active Material as a Function of Charge and Discharge Rate.

several empirical parameters. The constant 8.0 in Eq.(6) is a compressibility factor that scales the volume differential A in Fig. 2 for a given pressure differential P_d. The dependence of the integrated volume change on this scale factor is indicated in Fig. 5. A second empirical parameter in Eq.(6) is b_r, the time constant for relaxation from the high volume to the low volume forms of active material defined in Fig. 2 as functions of state of charge. The dependence of the integrated volume change on b_r is indicated in Fig. 6. Values for the other parameters used in the simulations of Figs. 5 and 6 are indicated in Table 1. As indicated in Fig. 5, the cumulative volume changes decrease linearly with the compressibility scale factor when this parameter is below about 10 $cc^{-1}psi^{-1}$. When this parameter is much greater than about 20 $cc^{-1}psi^{-1}$, very little cumulative volume change results from hydrogen pressure fluctuations, simply because the active material has become sufficiently incompressible to not be greatly affected by pressure fluctuations.

The results of Fig. 6 indicate that integrated or cumulative active material volume changes from hydrogen pressure fluctuations increase sharply as the time constant for relaxation of the high volume to the low volume forms of the active material (defined in Fig. 2) approaches the charge/discharge cycle time. The reason for this behavior is that when this time constant is large relative to the cycle time the active material remains in a high volume, highly compressible state during the entire cycle. Hydrogen pressure fluctuations will have the maximum impact on the volume of this low density state. Small time constants allow the high volume (low density) state to relax to a relatively incompressible material that exhibits minimal volume response to hydrogen pressure fluctuations.

The time constant b_a in Eq. (8) determines the rate at which pressure differentials between the interior of the active material deposit and the exterior applied pressure undergo equilibration. The dependence of the cumulative changes in active material volume on this time constant is indicated in Fig. 7. The other parameters used in the simulation of Fig. 7 are detailed in Table 1. When the time constant b_a is quite small relative to the cycle time, very little effect is observed on the integrated volume change because essentially no pressure differential is developed between the interior

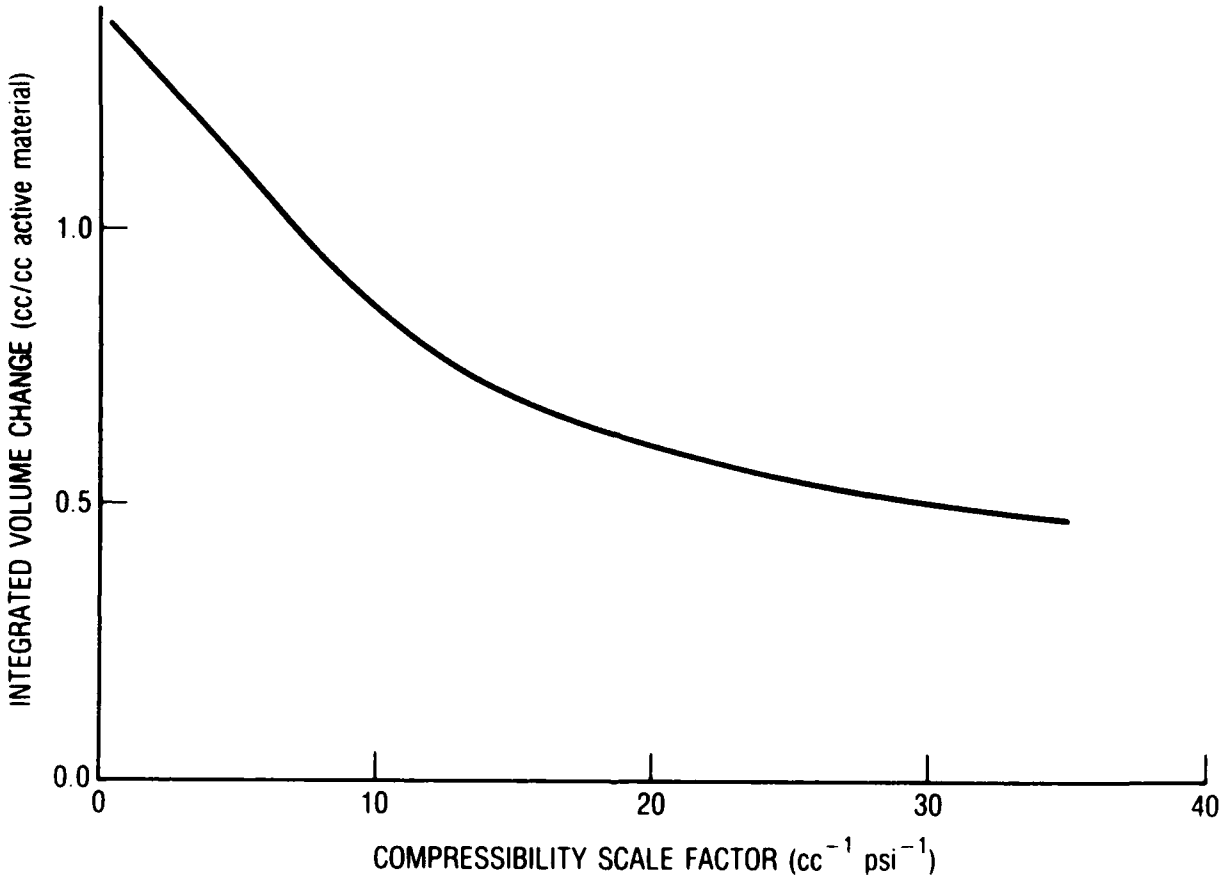

Figure 5. Integrated Volume Change for Nickel Electrode Active Material as a Function of the Compressibility Scale Factor in Eq. (6).

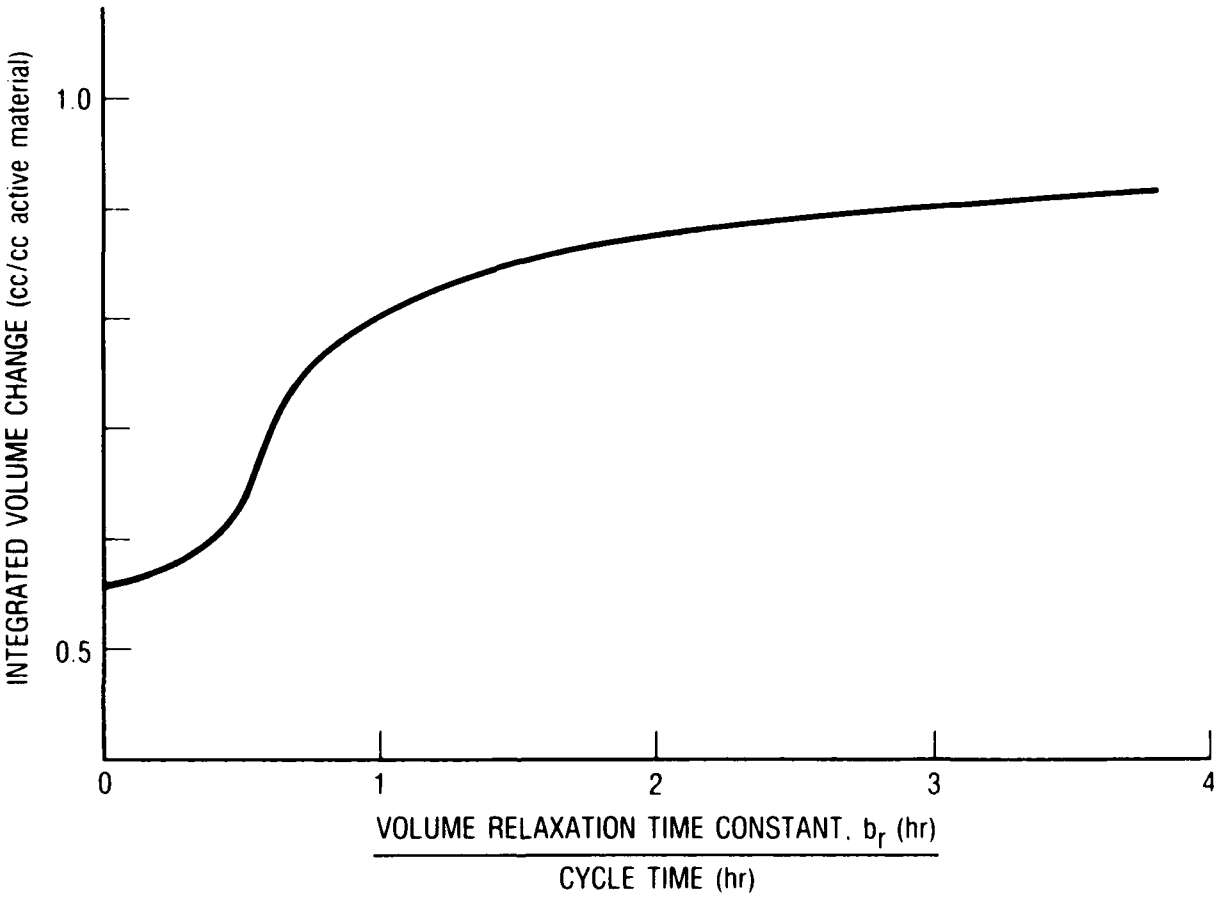

Figure 6. Integrated Change in Volume for Nickel Electrode Active Material as a Function of Time Constant for Relaxation of High Volume Form to Low Volume Form of Active Material in Fig. 2. Time constant is normalized to total charge/discharge cycle time.

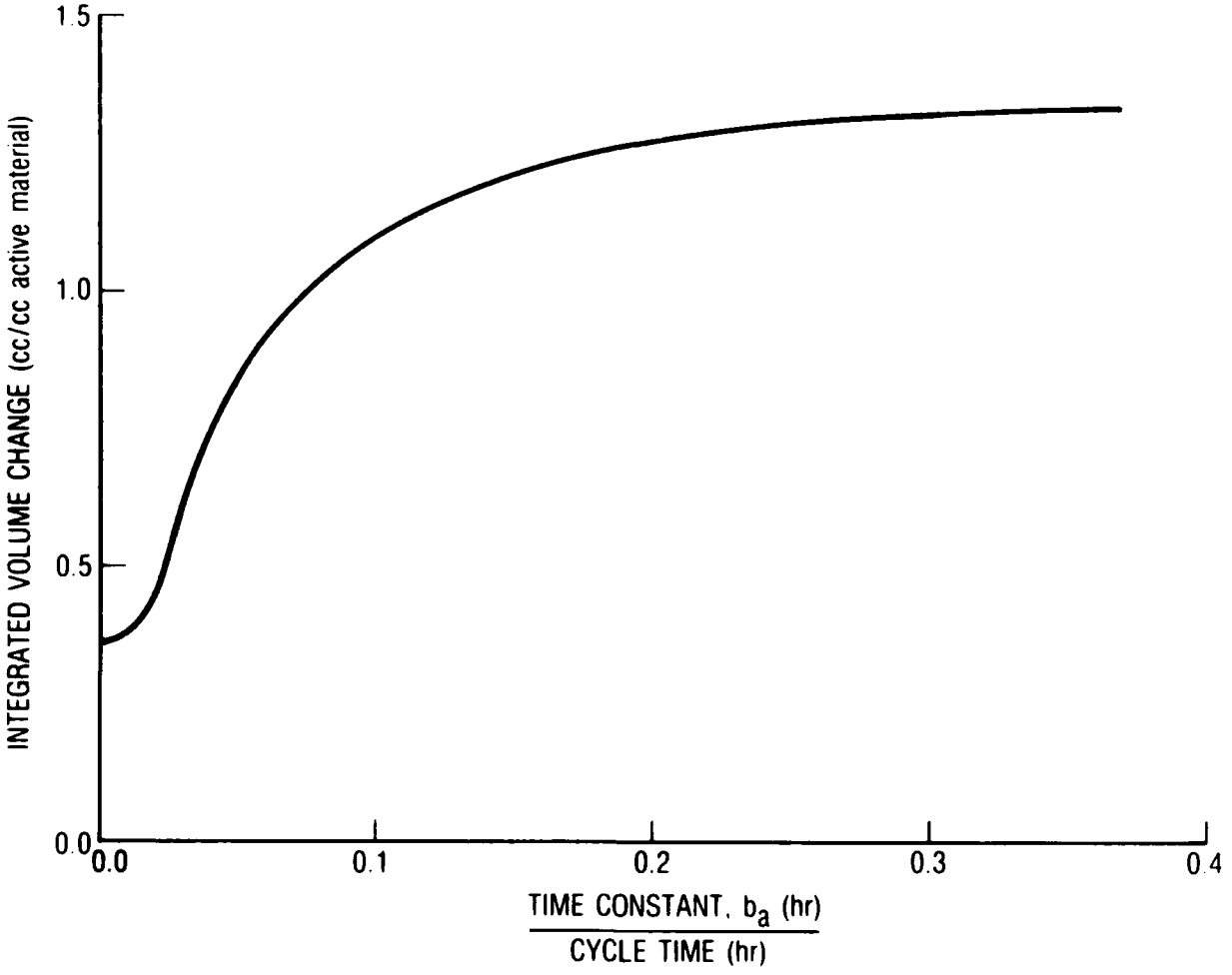

Figure 7. Integrated Change in Volume of Nickel Electrode Active Material as a Function of Time Constant for Pressure Equilibration Between the Interior and Exterior of the Active Material. Time constant is normalized to the total charge/discharge cycle time.

and the exterior of the active material. As the time constant increases, the integrated volume change increases dramatically until eventually it is limited by the volume available in the sinter for expansion. For large time constants b_a, the pressure differential across the active material can become very large and may cause active material to be forced from the pores of the sinter structure. For the conditions of operation examined in Fig. 7, such a situation begins to arise as b_a approaches 10% of the cycle time. The results of Fig. 7 indicate that the expansion and contraction of active material in nickel electrodes due to pressure fluctuations is quite sensitive to the rate at which gas can equilibrate within the active material deposit. While this rate will depend to some extent on the morphology of the deposit, the data reported in Ref. 1 indicate that typical time constants are on the order of minutes. A value of 6 minutes (0.1 hr) was chosen for most of the modeling reported here.

The final parameter that was felt to be potentially important in influencing cumulative volume changes induced in active material by pressure fluctuations was the maximum volume allowed for the high volume state of the active material, as defined in Fig. 2. This volume is limited to 0.62 cc/g by the volume typically available in a sintered electrode having active material loading of 1.6 g/cc void volume. Data from Ref. 1 indicate that for some operating conditions (particularly after high rate overcharge for cobalt containing material) the active material in its high volume state nearly fills the available void volume. Figure 8 shows how the cumulative volume change depends on the maximum volume that the active material can approach, V_i+A in Fig. 2. Also indicated in Fig. 8, the volume changes tend to increase linearly with the maximum allowed active material volume when this volume is above 0.40 cc/g. For maximum limiting volumes below 0.40 cc/g the compressibility of the active material begins to become limited by the volume of the low density form of the active material, which constitutes a relatively fixed lower volume limit. In this work it is assumed that the active material volume cannot be compressed to less than the volume of the hexagonal close packed nickel hydroxide structure, which has a volume of slightly more than 0.25 cc/g.

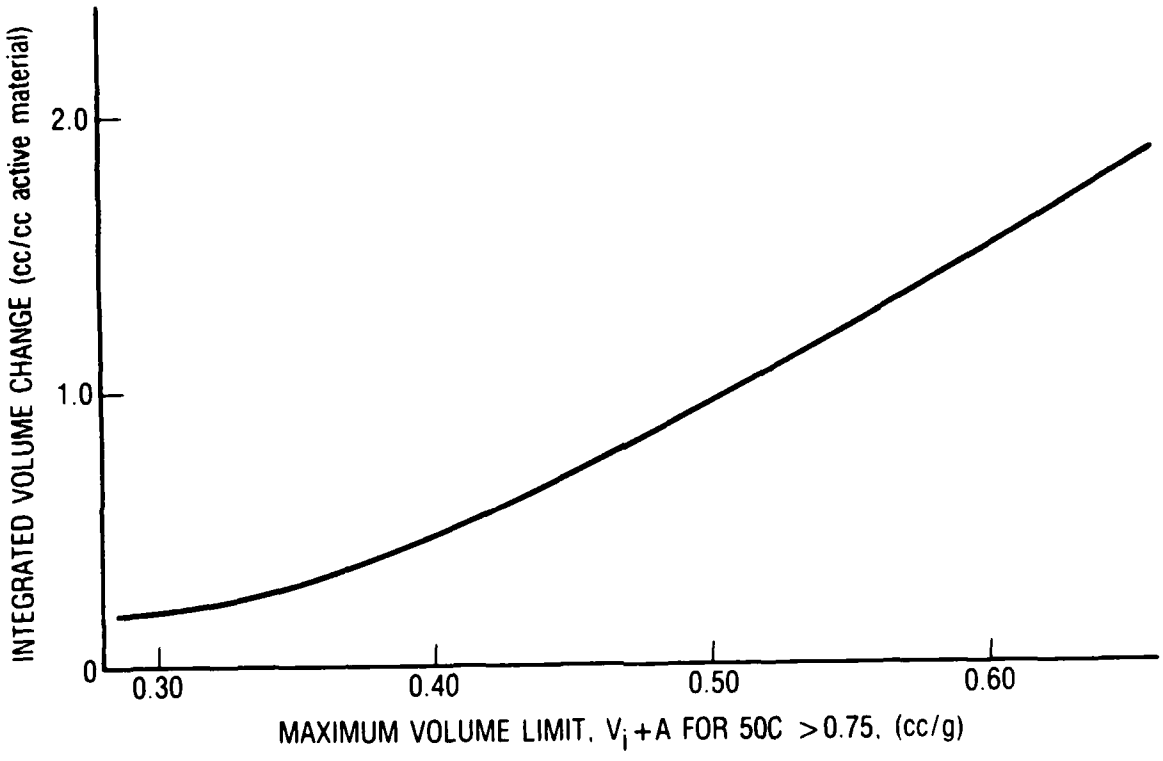

Figure 8. Integrated Change in Volume of Nickel Electrode Active Material as a Function of Maximum Volume for High Volume Form of Active Material in Fig. 2.

B. NICKEL-HYDROGEN CELL SIMULATIONS

The model described above has been used to simulate a number of different operational conditions for nickel-hydrogen cells. For each simulation a control simulation was also run in which the effect of the hydrogen pressure was eliminated, resulting in the active material volume changes arising only from the changes in state of charge as the cell is cycled (similar to the operation of a nickel-cadmium cell where comparatively little pressure is developed). The results of these simulations are indicated in Figs. 9-13. The parameters and conditions simulated in each of these cases are indicated in Table 2 for nickel-hydrogen cells that operate over a 1000-psi pressure range for full discharge. For simulation at depths of discharge less than 100%, the pressure cycle indicated in Fig. 1 was used with the inclusion of a pressure offset P_{off}, which corresponded to the cell pressure at the deepest depth of discharge (or lowest pressure point). Parameters other than those indicated in Table 2 were fixed for all simulations, and were: b_a = 0.1 hr, b_r = 24 hr, and A and V_i were, as indicated in Fig. 2, functions of state of charge.

Table 2. Simulation Conditions Used in Figures 9-13

	Fig 3	Fig 4	Fig 5	Fig 6	Fig 7
Orbit type	24 hr	24 hr	90 min	90 min	90 min
Depth of discharge	80%	40%	80%	40%	20%
t_c	16.0 hr	9.0 hr	0.75 hr	0.75 hr	0.75 hr
t_o	22.8 hr	22.8 hr	1.00 hr	1.00 hr	1.00 hr
t_d	24.0 hr	24.0 hr	1.50 hr	1.50 hr	1.50 hr
P_c	700 psi	300 psi	700 psi	300 psi	100 psi
P_m	800 psi	400 psi	800 psi	400 psi	200 psi
P_{off}	200 psi	600 psi	200 psi	600 psi	800 psi

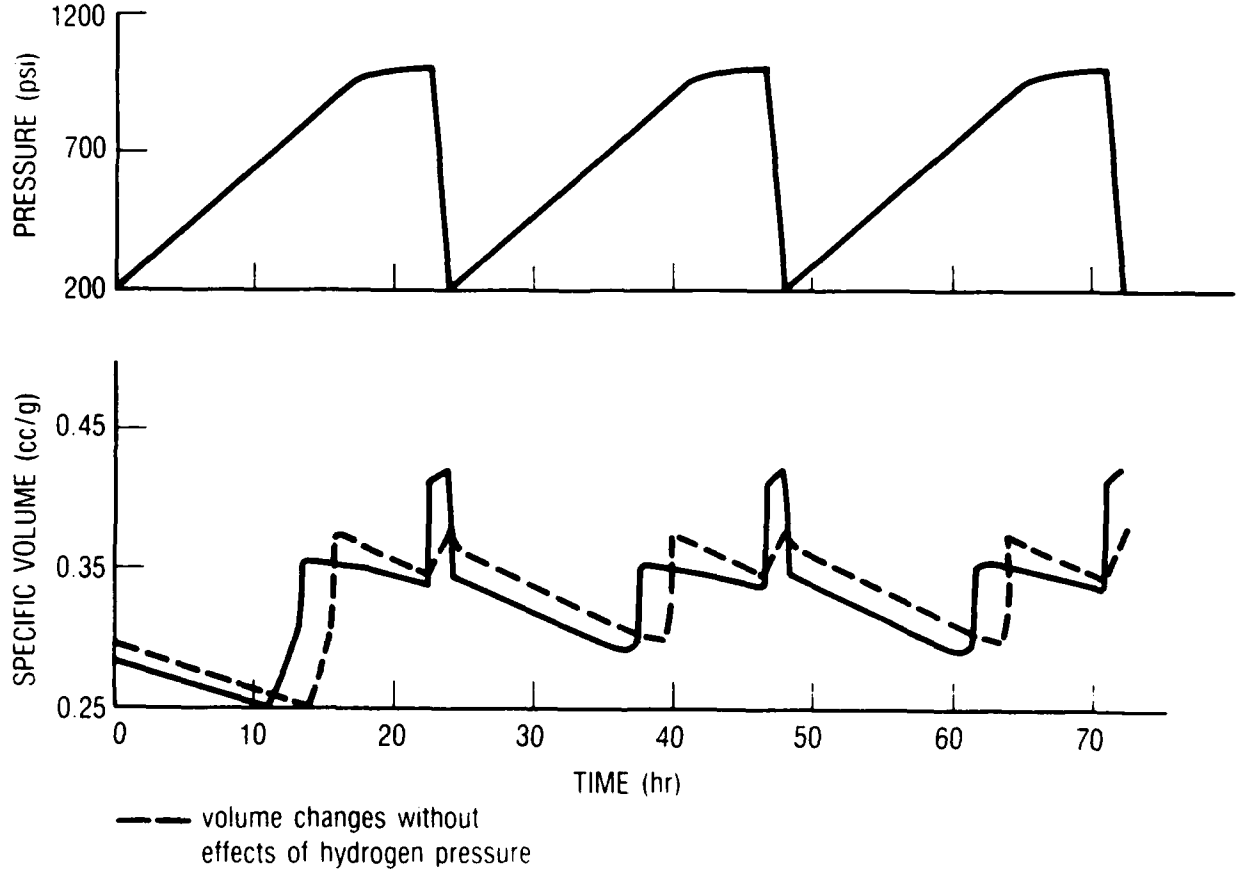

Figure 9. NiH_2 Cell Pressure and Active Material Volume Changes During Three Geosynchronous Cycles at 80% Depth of Discharge.

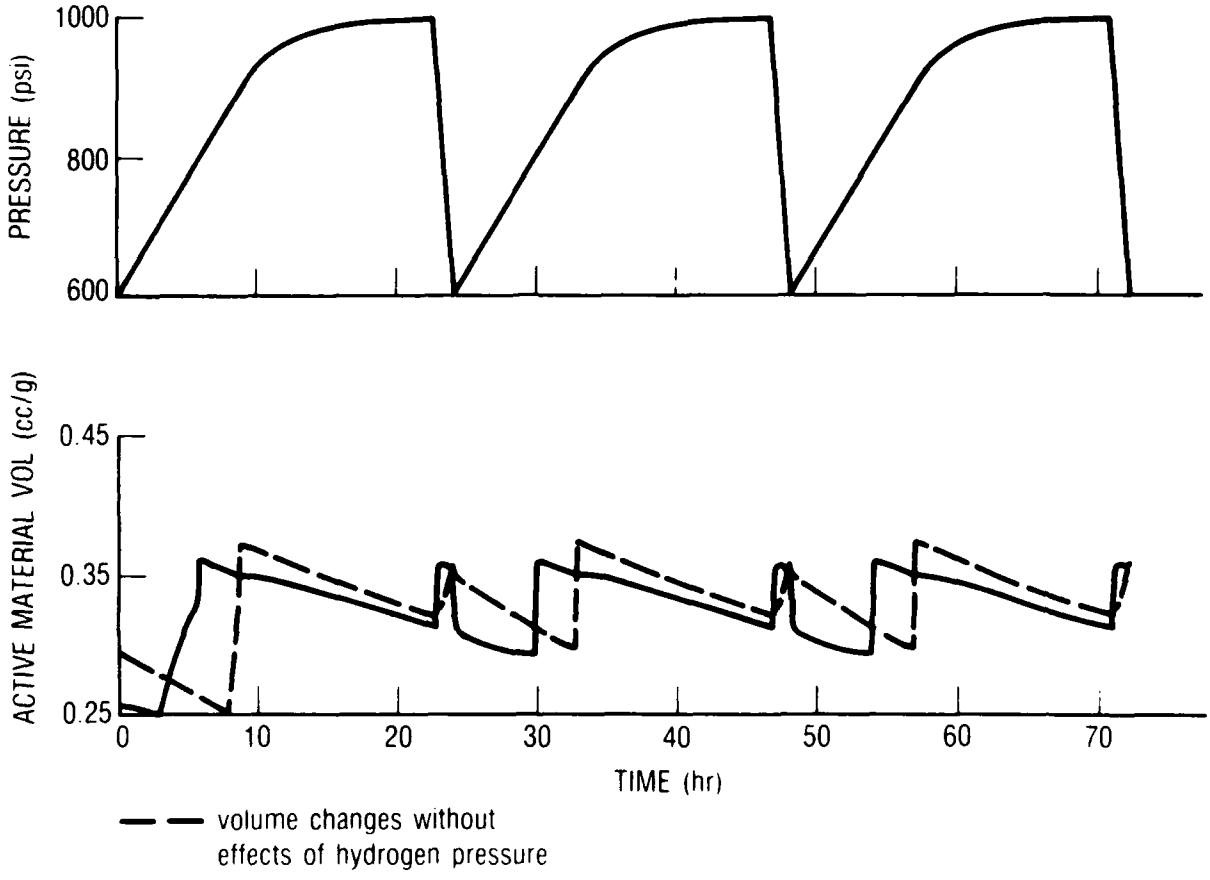

Figure 10. NiH_2 Cell Pressure and Active Material Volume Changes During Three Geosynchronous Cycles at 40% Depth of Discharge.

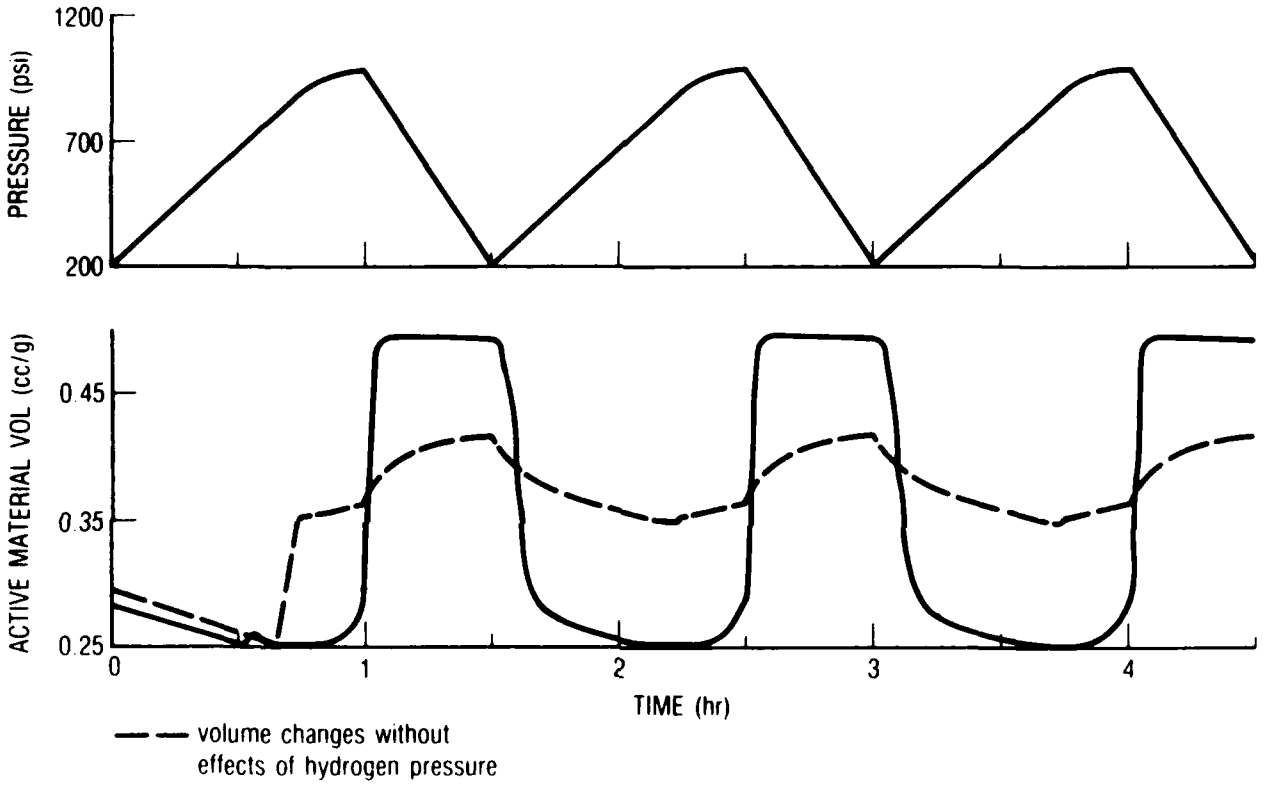

Figure 11. NiH_2 Cell Pressure and Active Material Volume Changes During Three Low Earth Orbit Cycles at 80% Depth of Discharge.

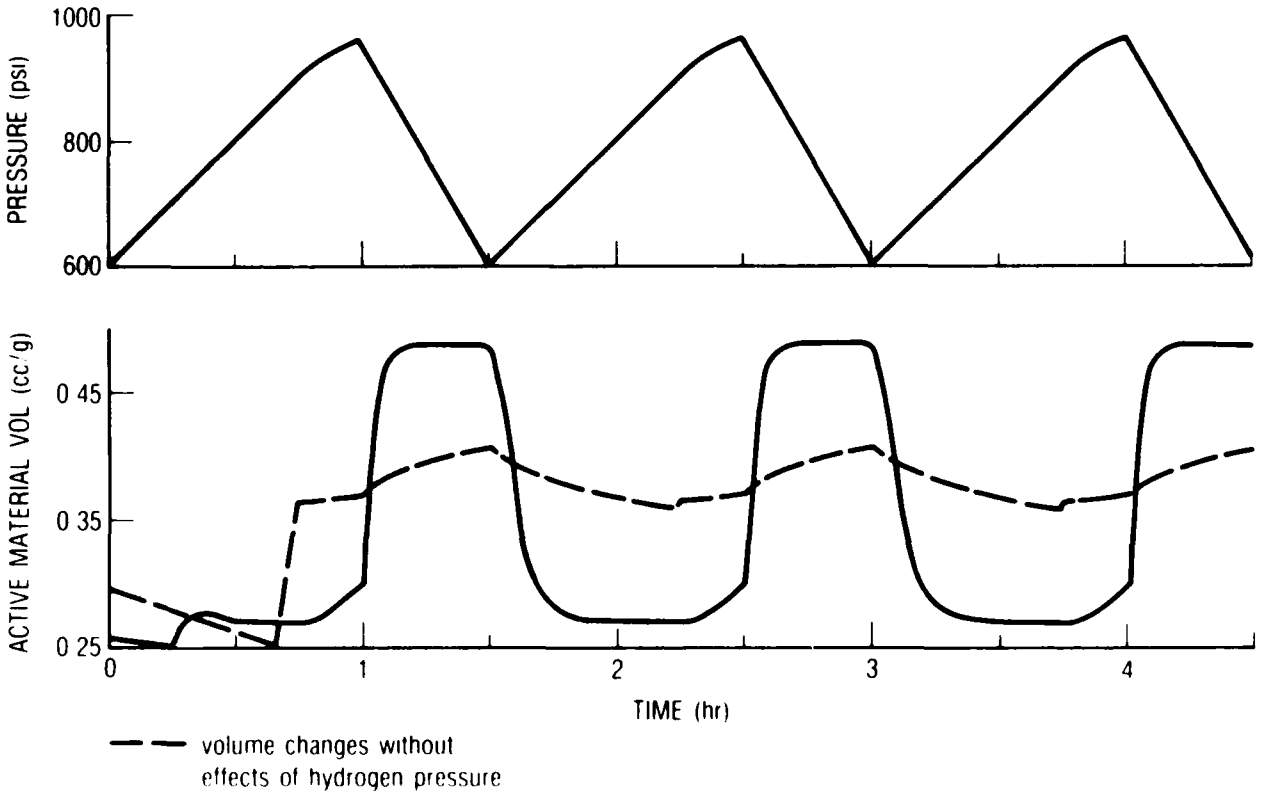

Figure 12. NiH_2 Cell Pressure and Active Material Volume Changes During Three Low Earth Orbit Cycles at 40% Depth of Discharge.

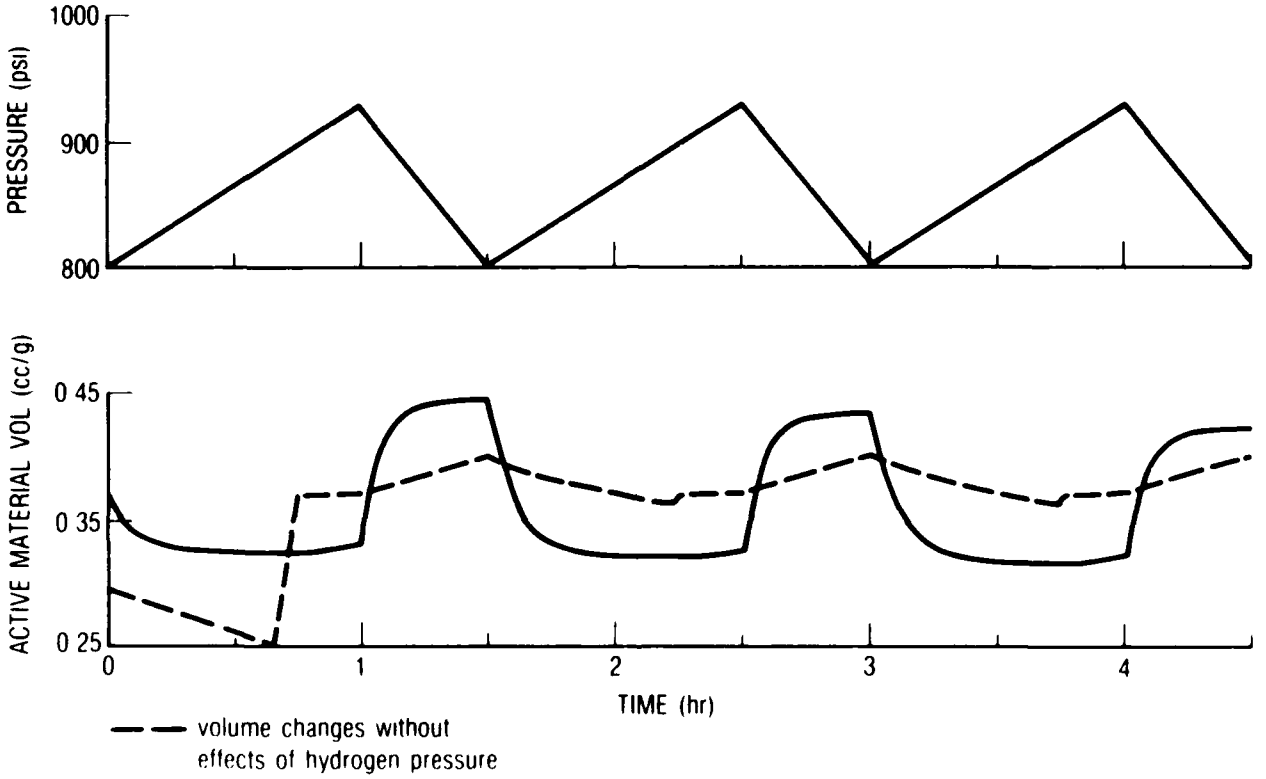

Figure 13. NiH_2 Cell Pressure and Active Material Volume Changes During Three Low Earth Orbit Cycles at 20% Depth of Discharge.

The results of Figs. 9 and 10 for 24-hr, or geosynchronous, orbits that have 72-min eclipse periods during which the batteries provide power, indicate that the major effect of hydrogen pressure in the nickel-hydrogen cells is limited to the discharge period. During discharge the pressure is changing much more rapidly than in other parts of the cycle. The active material volume changes due to changing hydrogen pressure are relatively small compared to those arising from the changing state of charge until the depth of discharge exceeds about 50%, beyond which increasingly significant changes in active material volume result from the rapidly decreasing pressure during discharge (see Fig. 9).

Figures 11-13 indicate the results of a series of simulations for nickel-hydrogen battery operation to support loads during eclipse in 90-min orbits, which correspond to a typical low-earth orbit. The simulations were done for various depths of discharge: 80%, 40%, and 20% for Figs. 11-13, respectively. These figures indicate that large changes in the volume of the active material of the nickel electrodes can be driven by the swings in pressure that occur during both charge and discharge. The periodic swing in active material volume increases rapidly with increasing depth of discharge, until at about 50% depth of discharge the volume swings become large enough that it is likely that some of the active material will be forced out of the sintered structure. The results of these simulations are reasonably consistent with results obtained from nickel-hydrogen cells that have been cycled over high depths of discharge. It is typical that the nickel electrodes from these cells have significant quantities of active material forced out of the sinter and onto the surface of the sintered substrate.

The stresses within the active material deposit of sintered nickel electrodes can cause movement of the active material, possible shedding from the electrode, isolation from the sinter surfaces, and possibly even damage to the sinter structure. All of these forms of electrode degradation are expected to be driven to some extent by the changes in the volume of the active material. Some indication of the cumulative driving forces over many cycles for degradation can be obtained by integrating the changes in the active material volume over many cycles. The results obtained without the effects of

hydrogen pressure are indicated in Fig. 14 for the five simulations indicated in Table 2. The results in Fig. 14 indicate that operation of nickel electrodes at 80% depth of discharge in a 24-hr orbit (or at 40% depth of discharge with significant overcharge) is considerably more stressful than the same number of cycles in a 90-min orbit. When it is realized that degradation from cadmium electrodes is not considered here, and that stress is likely to not be linearly proportional to volume changes (stress may be more dependent on active material displacement, which goes as the cube root of the volume change), the results in Fig. 14 are qualitatively consistent with nickel-cadmium battery performance in life-tests involving various cycling conditions.

The integrated volume changes over a 1000-cycle period are again indicated in Fig. 15 for nickel-hydrogen battery cells. The effects of the pressure changes that occur in the nickel-hydrogen cells have been included in the results of Fig. 15. Comparison of these results with those of Fig. 14 shows that the rapid cycling in low earth orbits is much more stressful on nickel electrodes in nickel-hydrogen cells than for nickel-cadmium cells, which do not experience rapid swings in pressure during cycling. The results in Fig. 15 also indicate that pressure stresses on nickel electrodes may result in significantly greater stresses on nickel electrodes in 24-hr orbits when depths of discharge greater than 50-60% are used for nickel-hydrogen batteries. Again these results are reasonably consistent with test results. Nickel-hydrogen cells in low earth orbit tests at high depths of discharge have tended to fail from breakdown of the nickel electrode structure after 10,000 cycles or less, well short of the cycle life that this electrode is projected to be capable of based on electrode testing in other cell environments. In 24-hour orbit testing nickel-hydrogen cells have performed quite well, with most nickel electrode failures arising after extended cycling at depths of discharge on the order of 80%.

The results discussed above demonstrate that pressure changes during the operation of nickel-hydrogen battery cells can produce forces that are capable of exerting high stresses on the nickel electrodes, and thus causing increased rates of nickel electrode degradation. Although the results of this study are

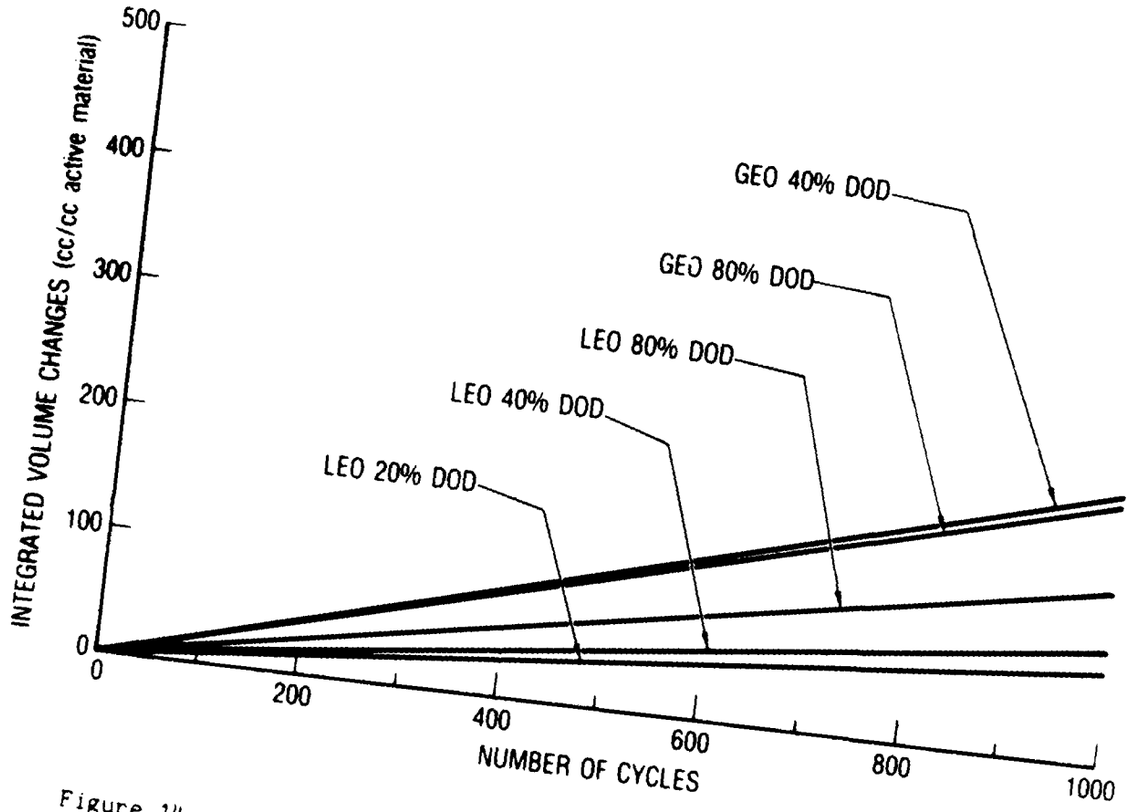

Figure 14. Integrated Volume Changes in Nickel Electrodes Due to Effects Other Than Applied Hydrogen Pressure for Various Orbital Uses.

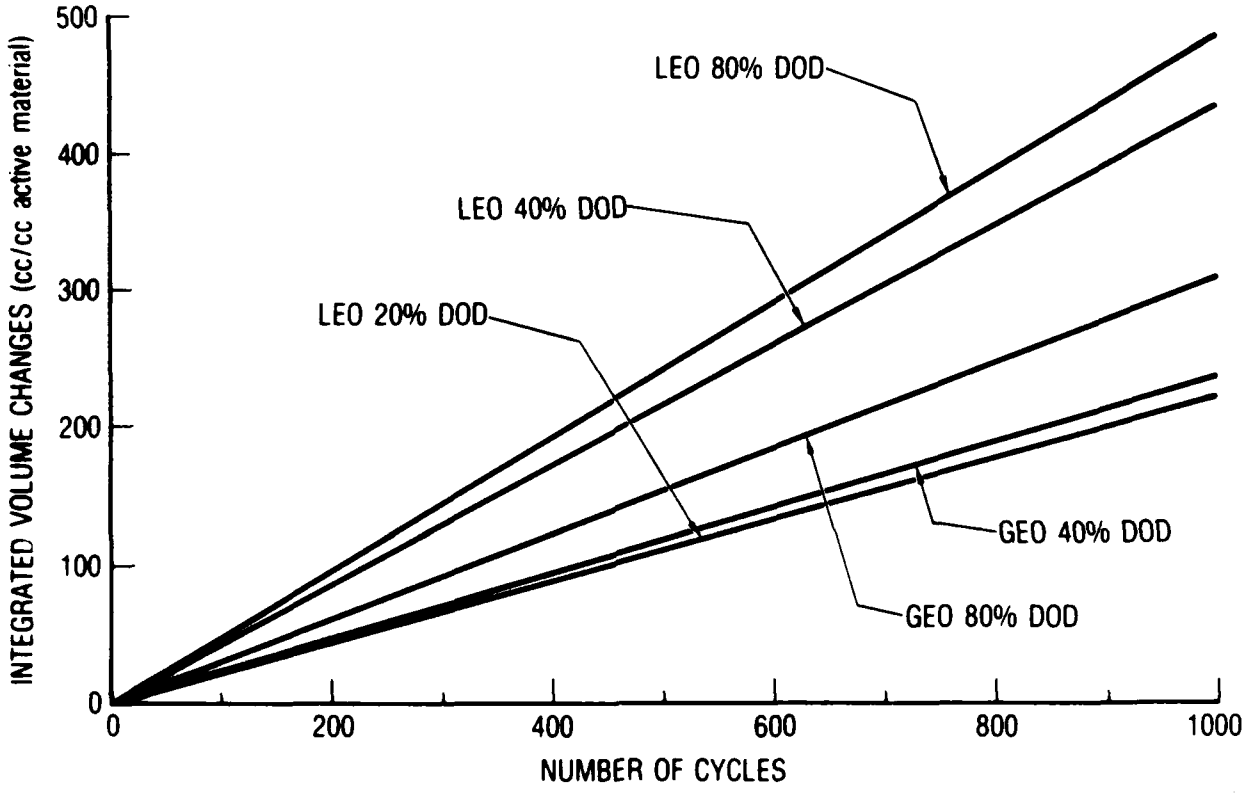

Figure 15. Integrated Volume Changes in Nickel Electrodes, Including Effects from Applied Hydrogen Pressure for Various Orbital Uses.

qualitatively consistent with the results from tests utilizing batteries with nickel electrodes, it is clear that many important variables are present in these batteries other than varying hydrogen pressure. An experimental test on an actual nickel-hydrogen cell could be done that would readily evaluate the importance of pressure fluctuations on nickel electrode performance during long term cycling. This test could, for example, involve two nickel-hydrogen cells operated electrically in a 90-min cycle. One cell would operate normally with large pressure variations, while the other cell could be connected to a large hydrogen reservoir so that pressure variations would be small. After extensive cycling, performance differences should develop, based on the results obtained here. The cell connected to the reservoir should exhibit significantly improved performance. Cell disassembly following the test would allow analysis of the relative changes in the nickel electrodes at a microscopic level and at a performance level to determine the degradation modes that were operative during the cycling.

IV. SUMMARY

Analysis has been done indicating that significant nickel electrode degradation due to pressure fluctuations is possible in nickel-hydrogen battery cells that operate over a wide dynamic pressure range. This degradation arises from compression and expansion of the active material deposits in the electrodes as the pressure periodically rises and falls while the cells are cycled. The expansion and contraction of the active materials have been modeled for cells operating at pressures up to 1000 psi. The degradation from these effects is projected to begin to become significant in geosynchronous applications utilizing high depths of discharge, and may become quite severe in low earth orbit applications that involve rapid cycling or high depth of discharge. Tests are proposed that are capable of evaluating the importance of nickel electrode degradation in nickel-hydrogen cells due to pressure cycling.

REFERENCES

1. A. H. Zimmerman and P. K. Effa, "Nickel Hydroxide Active Material Densities," The Aerospace Corporation, to be published.

2. D. H. Fritts, J. Electrochem. Soc. 129 (1982) 118.

3. A. H. Zimmerman, J. Power Sources 12(1984) 233.

LABORATORY OPERATIONS

The Aerospace Corporation functions as an "architect-engineer" for national security projects, specializing in advanced military space systems. Providing research support, the corporation's Laboratory Operations conducts experimental and theoretical investigations that focus on the application of scientific and technical advances to such systems. Vital to the success of these investigations is the technical staff's wide-ranging expertise and its ability to stay current with new developments. This expertise is enhanced by a research program aimed at dealing with the many problems associated with rapidly evolving space systems. Contributing their capabilities to the research effort are these individual laboratories:

Aerophysics Laboratory: Launch vehicle and reentry fluid mechanics, heat transfer and flight dynamics; chemical and electric propulsion, propellant chemistry, chemical dynamics, environmental chemistry, trace detection; spacecraft structural mechanics, contamination, thermal and structural control; high temperature thermomechanics, gas kinetics and radiation; cw and pulsed chemical and excimer laser development including chemical kinetics, spectroscopy, optical resonators, beam control, atmospheric propagation, laser effects and countermeasures.

Chemistry and Physics Laboratory: Atmospheric chemical reactions, atmospheric optics, light scattering, state-specific chemical reactions and radiative signatures of missile plumes, sensor out-of-field-of-view rejection, applied laser spectroscopy, laser chemistry, laser optoelectronics, solar cell physics, battery electrochemistry, space vacuum and radiation effects on materials, lubrication and surface phenomena, thermionic emission, photosensitive materials and detectors, atomic frequency standards, and environmental chemistry.

Computer Science Laboratory: Program verification, program translation, performance-sensitive system design, distributed architectures for spaceborne computers, fault-tolerant computer systems, artificial intelligence, microelectronics applications, communication protocols, and computer security.

Electronics Research Laboratory: Microelectronics, solid-state device physics, compound semiconductors, radiation hardening; electro-optics, quantum electronics, solid-state lasers, optical propagation and communications; microwave semiconductor devices, microwave/millimeter wave measurements, diagnostics and radiometry, microwave/millimeter wave thermionic devices; atomic time and frequency standards; antennas, rf systems, electromagnetic propagation phenomena, space communication systems.

Materials Sciences Laboratory: Development of new materials: metals, alloys, ceramics, polymers and their composites, and new forms of carbon; nondestructive evaluation, component failure analysis and reliability; fracture mechanics and stress corrosion; analysis and evaluation of materials at cryogenic and elevated temperatures as well as in space and enemy-induced environments.

Space Sciences Laboratory: Magnetospheric, auroral and cosmic ray physics, wave-particle interactions, magnetospheric plasma waves; atmospheric and ionospheric physics, density and composition of the upper atmosphere, remote sensing using atmospheric radiation; solar physics, infrared astronomy, infrared signature analysis; effects of solar activity, magnetic storms and nuclear explosions on the earth's atmosphere, ionosphere and magnetosphere; effects of electromagnetic and particulate radiations on space systems; space instrumentation.

END

10-87

DTIC